

1 **Hybrid zone dynamics under weak Haldane's rule**

2 Ren-Xue Wang

3 BC Cancer Research Centre, BC Cancer Agency, Vancouver, British Columbia, Canada

4

5 *Running title: Wang, Hybrid zone dynamics under weak Haldane's rule*

6

7 *Correspondence:* Ren-Xue Wang, BC Cancer Research Centre, BC Cancer Agency,

8 675 West 10th Avenue, Vancouver, British Columbia, Canada V5Z 1L3. e-mail:

9 rwang@bccrc.ca. Phone: (604) 675 8000, extension: 7709. Fax: (604) 675 8185.

10

11 **The ability of genetic isolation to block gene flow plays a key role in the speciation of**
12 **sexually reproducing organisms. This paper analyses the hybrid zone dynamics affected**
13 **by “weak” Haldane’s rule, namely the incomplete hybrids inferiority**
14 **(sterility/inviability) against the heterogametic (*XY* or *ZW*) sex caused by a Dobzhansky-**
15 **Muller incompatibility. Different strengths of incompatibility, dispersal and density-**
16 **dependent regulation are considered; and the gene flow and clinal structures of allele**
17 **frequencies in the presence of short-range dispersal (the stepping-stone model) are**
18 **examined. I show that a weak heterogametic hybrid incompatibility could constitute a**
19 **substantial barrier that could reduce gene flow and result in non-coincident and**
20 **discordant clines of alleles. It is found that the differential gene flow is more**
21 **pronounced under a stronger density-dependent regulation. This study provides a**
22 **mechanistic explanation for how an adaptive mutation, which may only have a marginal**
23 **fitness effect, could set a gene up as an evolutionary hot-spot.**

24

25 **Keywords:** Dobzhansky-Muller incompatibility, Gene flow, Haldane's rule, Hybrid
26 sterility, Hybrid inviability, Hybrid zone, Speciation.

27

28 Hybrids between closely related species of sexually reproduced organisms generally suffer
29 from poor fertility or viability. The question puzzled Darwin himself when formulating his
30 theory of evolution by natural selection was how evolution could maintain inheritable
31 changes to cause hybrid sterility or inviability. Several decades had passed since Bateson
32 (Bateson, 1909, Orr, 1996), Dobzhansky (Dobzhansky, 1937) and Muller (Muller, 1940,
33 Muller, 1942) articulated the evolutionary mechanism that produces such hybrid
34 incompatibility; it is through a process of the establishment of epistatic deficiencies between
35 diverging populations. Detrimental epistasis can be accumulated over time by genetic drifts
36 and/or adaptive mutations in separated populations (Wittbrodt et al., 1989, Ting et al., 1998,
37 Barbash et al., 2003, Presgraves et al., 2003, Brideau et al., 2006, Masly et al., 2006, Phadnis
38 & Orr, 2009) without facing negative selection or “adaptive valley” (Wright, 1988, Gavrilets,
39 1997). When hybridization occurs, such epistatic interaction could cause sterility or
40 inviability. For instance, from a diallelic ancestral population, an *aabb* genotype could evolve
41 into *AAbb* and *aaBB* genotypes respectively in two separate subpopulations, where the “*A*” or
42 “*B*” allele faces little or no negative selection for their establishment. If “*A*” and “*B*” alleles
43 are incompatible with each other and hybridization occurs, hybrids carrying *AaBb* genotype
44 will become inferior. This form of reproductive barriers is thus dubbed Dobzhansky-Muller
45 (DM) isolation.

46 Haldane's rule represents a major form of BDM isolation in early speciation (Coyne &
47 Orr, 1989, Wu & Davis, 1993, Laurie, 1997). Haldane's rule indicates that hybridization of
48 closely-related species almost always produces sterile or inviable F_1 offspring of the
49 heterogametic sex (male in *XY* sex determination and female in *ZW* determination) as
50 opposed to those of the homogametic sex if they are sex-biased. This rule is widely present in
51 almost all taxa investigated (Coyne & Orr, 1998), including mammals, fruit flies, butterflies,
52 birds and many other animals, and dioecious plants (Coyne & Orr, 1989, Wu & Davis, 1993,

53 Laurie, 1997). Heterogametic hybrid sterility/inviability appears to be a critical intermediate
54 step during speciation of many species. However, little is known about the role of a
55 heterogametic hybrid incompatibility in affecting population dynamics (Wang, 2003, Wang
56 & Zhao, 2008). Sex-biased BDM isolation is often the first appeared and a common (if not
57 the most common) form of reproductive isolation in many closely related species pairs, but
58 they have been rarely considered in the theoretical models of speciation with gene flow. The
59 existing theoretical studies on the divergence-with-gene-flow are mainly on the interplays
60 between prezygotic isolation (sexual selection) and ecological differentiations (Dieckmann &
61 Doebeli, 1999, Arnegard & Kondrashov, 2004, Gourbiere, 2004, Van Doorn, 2004, van
62 Doorn et al., 2009, also see Coyne & Orr, 2004, Fitzpatrick et al., 2008, Fitzpatrick et al.,
63 2009).

64 Hybrid zone analysis provides an excellent system for appreciating the role of Haldane's
65 rule in population dynamics during speciation (Wang & Zhao, 2008). Theoretical studies on
66 BDM isolation in affecting gene flow and population dynamics were first attempted by
67 Barton & Bengtsson (1986) and Gavrilets (1997). Using heuristic approximation, Bengtsson
68 and Barton (Barton & Bengtsson, 1986) developed a hybrid zone model with BDM isolation
69 and made a first attempt to analyse the neutral gene flow in such a scenario. It was concluded
70 that in the presence of autosome-linked BDM isolation, neutral gene flow could be reduced
71 greatly, but only when it was closely linked to one of the selected alleles. BDM isolation can
72 only constitute a strong barrier to neutral alleles in a hybrid zone when most of them are
73 closely linked to loci under selection (Barton & Bengtsson, 1986). By adapting a more
74 sophisticated fitness matrix, Gavrilets (Gavrilets, 1997) extended the analysis and concluded
75 that epistatic BDM isolation can build up a very strong barrier to neutral gene flow. Gavrilets
76 described in greater detail of the properties of hybrid zones under BDM selection, such as the
77 shapes of clines in relation to strength of selection, migration and linkage. Both of these

78 models (Barton & Bengtsson, 1986, Gavrillets, 1997) use numerical approximations when
79 analysing diallelic, autosome-linked epistatic selection. Sex chromosome-linked and sex
80 dependent selection was not considered.

81 Recently, Wang and Zhao (Wang & Zhao, 2008) developed a recursion model to analyse
82 hybrid zone structure and gene flow in a more sophisticated scenario – sex-dependent and
83 sex-chromosome-linked BDM isolation. Different from the earlier hybrid zone models under
84 BDM isolation (Barton & Bengtsson, 1986, Gavrillets, 1997), this model provides a more
85 accurate account of the effects of BDM isolation in hybrid zone dynamics. Wang and Zhao's
86 model (Wang & Zhao, 2008) separately considers the loci of *X*, *Y*, incompatible autosomes,
87 and neutral autosomes. The model allows the analysis of various alleles in a hybrid zone both
88 temporally and spatially. The analysis shows that in the presence of short-range dispersal
89 (stepping-stone model), a sex-biased hybrid incompatibility is an efficient barrier that
90 impedes gene flow across hybrid zones. Sex-biased hybrid incompatibilities differ from each
91 other depending on the sex that they select against, and the chromosomes where the
92 incompatible alleles are localized (Wang & Zhao, 2008).

93 The current paper focuses on the effects of “weak” Haldane's rule or the partial sex-biased
94 incompatibility that only causes inferiority of one sex in a fraction of carriers ranging from 0
95 to 100%. Between populations, weak sterility and inviability can arise as incidental
96 byproducts of divergence, such as adaptive mutations or genetic drifts, which may not be
97 readily observable in field and laboratory investigations. However, the population dynamics
98 under such otherwise unnoticeable partial isolation may be important for the formation of
99 Haldane's rule (Wang, 2003, Wang & Zhao, 2008). Many questions can be asked, such as,
100 how efficient a weak incompatibility could be as a genetic barrier; and to what extent it does
101 affect gene flow and hybrid zone structure; or how it is related to other factors in a hybrid
102 zone. The dynamics of such system may provide insights for understanding the evolutionary

103 mechanisms underlying speciation and Haldane's rule. Here, I quantitatively analyze the
104 influence of such partial incompatibility on the effective dispersal, density distribution, and
105 clinal structure of alleles across a hybrid zone. Variables that are considered also include
106 dispersal and density-dependent regulation.

107

108 **Definitions and assumptions**

109 Some common assumptions of population genetics are adopted. These include random
110 mating, discrete and non-overlapping generations, finite parental populations and passage of
111 alleles between generations at their probabilities (Endler, 1973, Slatkin, 1973). The parental
112 populations (H_1 and H_2 in the text, Wang & Zhao, 2008) are geographically separated and
113 genetically distinct.

114 *Sex-biased, two-locus BDM incompatibility.* Assume that between two diverging
115 populations, there is inferiority (sterility or inviability) that affects only hybrids of the
116 heterogametic sex. This is caused by detrimental epistatic interaction between two loci (two-
117 locus BDM incompatibility). The two incompatible alleles are localized on the sex
118 chromosome X_1 and an autosome A_2 , which originate from different populations. These
119 alleles cause no fitness loss in their parental populations. The strength of an X_1A_2
120 incompatibility (ψ) ranges from 0 to 1, namely that between 0 and 100% of the carriers of a
121 specific sex are inferior (sterile or inviable). I assume that hybrid inferiority is a continuous
122 quantitative trait – each incompatibility causes a fitness loss and produces fewer offspring in
123 average in accordance with its strength ($0 \leq \psi \leq 1$). The rest of the alleles are selectively
124 neutral and confer no fitness effects (loss or gain) in hybrids. In a deme, a fraction of hybrids
125 of affected sex are eliminated according to the strength of incompatibility. All other progeny
126 are equally fit, but subject to further segregation in later generations. For simplicity, we

127 assume male heterogamety (XY) but the results should apply to female heterogametic (ZW)
128 species as well.

129 *Density dependent regulation (r)*. In this study, density dependent regulation (r) is defined
130 as the ability of a population to adjust its size toward its carrying capacity (N_0). The effect of
131 a hybrid incompatibility is not density dependent (see below). However, the reduction of the
132 size caused by the incompatibility leads to a recovery of the deme toward its carrying
133 capacity.

134 *Gene flow and effective dispersal/migration*. Bengtsson (1985) has provided a clear
135 definition of effective dispersal/migration, “The effective migration rate, m_e , is that rate of
136 migration which would have the same evolutionary effect in a population with no genetic
137 barrier as the actual migration rate now has in the population with a barrier.” For short-term
138 dispersal in the stepping stone model (Endler, 1973), dispersal only occurs between
139 neighbouring demes by a dispersal rate λ . I consider the rate of an allele entering the opposite
140 population across the zone as the “evolutionary effect (Bengtsson, 1985)”. The effective
141 dispersal λ_e is defined as the equivalent dispersal under no genetic isolation ($\psi = 0$) that could
142 achieve the same gene flow (the rate of an allele entering the opposite population) in a
143 scenario with a genetic incompatibility ($0 \leq \psi \leq 1$). In other words, the effective
144 dispersal/migration λ_e is the product of λ multiplied with the ratio of the rate of an allele
145 entering the opposite population in the presence of a genetic barrier (when $0 \leq \psi \leq 1$) to that
146 rate in the absence of a genetic barrier (when $\psi = 0$).

147 The meaning of the effective dispersal (λ_e) is the same as that the effective migration (m_e)
148 defined by (Bengtsson, 1985)(Barton & Bengtsson, 1986), and Gavrillets (Gavrillets, 1997).
149 However, Barton and Bengtsson (Barton & Bengtsson, 1986) and Gavrillets (Gavrillets, 1997)

150 only considered the flow of neutral markers. In this analysis, the flow of different alleles (*X*-
151 linked, *Y*-linked, incompatible autosomal, and neutral autosomal) are considered separately.

152 **Model**

153 The Wang and Zhao's recursion model for short-range dispersal (Wang & Zhao, 2008) is
154 extended for examining the influences of weak incompatibilities on hybrid zone dynamics. I
155 use the stepping-stone model for short-range dispersal (Endler, 1973, Wang & Zhao, 2008).
156 Briefly upon a scenario of secondary contact, a hybrid zone consisting of a chain of “*n*”
157 demes of equal size is formed by migration of both parental populations (H_1 to H_2 , see Wang
158 & Zhao, 2008); and the migration of mature adults occurs between adjacent demes. In every
159 generation, each deme loses λ ($0 \leq \lambda \leq 0.5$) of its offspring to migration and at the same time
160 it receives input migration of λ from the adjacent demes ($\lambda/2$ on each side). In the either end
161 of the chain, the deme exchanges migrants with the corresponding parental population. The
162 size of each parental population is 100 times that of the hybrid zone.

163 Four independently localized loci, each with two alleles are considered and denoted X_1/X_2 ,
164 Y_1/Y_2 , A_1/A_2 and C_1/C_2 . All these genotypes are expressed as $X_iX_jA_kA_lC_oC_p$ for females and
165 $X_iY_jA_kA_lC_oC_p$ for males, where i , k , and o represent the maternal origin alleles and j , l , and p
166 represent the paternal origin alleles. This diallelic system consists of $4^3 = 64$ possible
167 genotypic combinations of offspring for each sex (Wang & Zhao, 2008). Throughout the
168 paper, the subscripts 1 and 2 represent the population origin of alleles.

169 The frequency of each genotypic combination of either a sperm or an egg produced in
170 generation t is expressed as $p_{X_rA_sC_z}^{(t)sperm}$, $p_{Y_rA_sC_z}^{(t)sperm}$ and $p_{X_qA_sC_w}^{(t)egg}$, where q , r , s , t , w , or z represents the
171 population origin of the allele (1 or 2). Accordingly, the frequency of a given genotypic
172 combination in generation t in a hybridizing deme is the product of frequencies of a sperm
173 and an egg (Wang & Zhao, 2008) where:

174
$$\mathbf{u}^{(t)} = P_{X_q Y_r A_s A_t C_w C_z}^{(t)} = P_{X_q A_s C_w}^{(t)egg} \bullet P_{Y_r A_t C_z}^{(t)sperm} \quad (1)$$

175 or

176
$$\mathbf{v}^{(t)} = P_{X_q X_r A_s A_t C_w C_z}^{(t)} = P_{X_q A_s C_w}^{(t)egg} \bullet P_{X_r A_t C_z}^{(t)sperm} \quad (2)$$

177 The $\mathbf{u}^{(t)}$ or $\mathbf{v}^{(t)}$ represents the frequency of a genotype $X_q Y_r A_s A_t C_w C_z$ or $X_q X_r A_s A_t C_w C_z$ in males
 178 or females in generation t before migration respectively.

179 The frequencies of genotypic combinations for each sex in a chain of demes in generation
 180 t are expressed by $(n \times m)$ matrices ($m = 64$), $U_0^{(t)}$ (for male) and $V_0^{(t)}$ (for female).

181
$$U_0^{(t)} = \begin{bmatrix} u_{11}^{(t)} & \cdots & u_{1m}^{(t)} \\ \vdots & & \vdots \\ \vdots & & \vdots \\ u_{n1}^{(t)} & \cdots & u_{nm}^{(t)} \end{bmatrix} \quad \text{and} \quad V_0^{(t)} = \begin{bmatrix} v_{11}^{(t)} & \cdots & v_{1m}^{(t)} \\ \vdots & & \vdots \\ \vdots & & \vdots \\ v_{n1}^{(t)} & \cdots & v_{nm}^{(t)} \end{bmatrix} \quad (3)$$

182 in which each row vector represents the frequencies of genotype combinations in deme i
 183 computed by (1) or (2). The range of i is between 1 to n corresponding to the positions of
 184 demes and the range of j is between 1 to m ($m = 64$ in this four loci scenario) corresponding
 185 to genotypic combinations.

186 The size of a compatible genotypic combination in deme i is thus:

187
$$w_{ij}^{(t)} = N_i^{(t-1)} u_{ij}^{(t)} \quad \text{and} \quad z_{ij}^{(t)} = N_i^{(t-1)} v_{ij}^{(t)} \quad (4)$$

188 The size of an incompatible genotypic combination in deme i is:

189
$$w_{ij}^{(t)} = (1 - \psi) N_i^{(t-1)} u_{ij}^{(t)} \quad \text{and} \quad z_{ij}^{(t)} = (1 - \psi) N_i^{(t-1)} v_{ij}^{(t)} \quad (5)$$

190 Here, ψ ($0 \leq \psi \leq 1$) is the strength of an incompatibility. A ψ fraction of an incompatible
 191 genotype will be inferior and eliminated in the deme; $(1 - \psi)$ will survive.

192 The density-dependent regulation of the population/deme size is based on the classic
 193 logistic model of population growth (see Hartl & Clark, 1997, page 31) and its strength is

194 expressed as r (the intrinsic rate of increase). When the male is the affected sex, the size of
 195 deme i in generation t before migration is calculated by:

$$196 \quad N_i^{(t)} = \sum_j^m w_{ij}^{(t)} + r \sum_j^m w_{ij}^{(t)} \left(1 - \frac{\sum_j^m w_{ij}^{(t)}}{N_0} \right) \quad (6)$$

197 When the female is the affected sex, the size of deme i is:

$$198 \quad N_i^{(t)} = \sum_j^m z_{ij}^{(t)} + r \sum_j^m z_{ij}^{(t)} \left(1 - \frac{\sum_j^m z_{ij}^{(t)}}{N_0} \right) \quad (7)$$

199 Here, N_0 is the carrying capacity or the optimal population size. In each generation before
 200 migration, the size of a population will be regulated by r until the balance is reached to satisfy

$$201 \quad N^{(t)} = N^{(t-1)} + rN^{(t-1)} \left(1 - \frac{N^{(t-1)}}{N_0} \right) \text{ (Hartl \& Clark, 1997). The } r \text{ and } \psi \text{ together determine the}$$

202 deme size.

203 The relative density of a deme before migration is:

$$204 \quad \rho = N_n^{(t)} / N_0 \quad (8)$$

205 Here, ρ is $0 \leq \rho \leq 1$ and N_0 is the carrying capacity, which is the same for all demes here.

206 The proportional sizes of genotypic combinations that will remain in the original demes

207 after elimination of incompatible offspring are:

$$208 \quad W^{(t)} = (1-\lambda) \begin{bmatrix} w_{11}^{(t)} & \cdots & w_{1m}^{(t)} \\ \vdots & & \vdots \\ \vdots & & \vdots \\ w_{n1}^{(t)} & \cdots & w_{nm}^{(t)} \end{bmatrix} \text{ and } Z^{(t)} = (1-\lambda) \begin{bmatrix} z_{11}^{(t)} & \cdots & z_{1m}^{(t)} \\ \vdots & & \vdots \\ \vdots & & \vdots \\ z_{n1}^{(t)} & \cdots & z_{nm}^{(t)} \end{bmatrix} \quad (9)$$

209 The proportional sizes of genotypic combinations that will be migrating in the direction from

210 H_1 to H_2 are:

$$211 \quad W_{mig1}^{(t)} = \frac{\lambda}{2} \begin{bmatrix} N_0 & 0 & \dots & 0 \\ w_{11}^{(t)} & w_{12}^{(t)} & \dots & w_{1m}^{(t)} \\ \vdots & \vdots & \vdots & \vdots \\ w_{(n-1)1}^{(t)} & w_{(n-1)2}^{(t)} & \dots & w_{(n-1)m}^{(t)} \end{bmatrix} \quad \text{and} \quad Z_{mig1}^{(t)} = \frac{\lambda}{2} \begin{bmatrix} N_0 & 0 & \dots & 0 \\ z_{11}^{(t)} & z_{12}^{(t)} & \dots & z_{1m}^{(t)} \\ \vdots & \vdots & \vdots & \vdots \\ z_{(n-1)1}^{(t)} & z_{(n-1)2}^{(t)} & \dots & z_{(n-1)m}^{(t)} \end{bmatrix} \quad (10)$$

212 Here, the first row represents the inputs from H_1 with the genotypes $X_1X_1A_1A_1C_1C_1$ for the
 213 female and $X_1Y_1A_1A_1C_1C_1$ for the male. The sum of frequencies of either sex equals to 1. We
 214 assume that the carrying capacity (N_0) is the maximum deme size. The proportional sizes of
 215 genotypic combinations that will be migrating in the direction from H_2 to H_1 are:

$$216 \quad W_{mig2}^{(t)} = \frac{\lambda}{2} \begin{bmatrix} w_{21}^{(t)} & \dots & w_{2(m-1)}^{(t)} & w_{2m}^{(t)} \\ \vdots & \vdots & \vdots & \vdots \\ w_{n1}^{(t)} & \dots & w_{n(m-1)}^{(t)} & w_{nm}^{(t)} \\ 0 & \dots & 0 & N_0 \end{bmatrix} \quad \text{and} \quad Z_{mig2}^{(t)} = \frac{\lambda}{2} \begin{bmatrix} z_{21}^{(t)} & \dots & z_{2(m-1)}^{(t)} & z_{2m}^{(t)} \\ \vdots & \vdots & \vdots & \vdots \\ z_{n1}^{(t)} & \dots & z_{n(m-1)}^{(t)} & z_{nm}^{(t)} \\ 0 & \dots & 0 & N_0 \end{bmatrix} \quad (11)$$

217 Here, the last row represents the inputs from H_2 with the genotypes $X_2X_2A_2A_2C_2C_2$ for the
 218 female and $X_2Y_2A_2A_2C_2C_2$ for the male.

219 Therefore, the proportional sizes of genotypic combinations in the zone after migration
 220 are:

$$221 \quad M_{mig}^{(t)} = W^{(t)} + W_{mig1}^{(t)} + W_{mig2}^{(t)} \quad \text{and} \quad F_{mig}^{(t)} = Z^{(t)} + Z_{mig1}^{(t)} + Z_{mig2}^{(t)} \quad (12)$$

222 Thus, the frequency of a genotype combination after migration will be:

$$223 \quad \omega_j^{(t)} = \frac{(1-\lambda)w_j^{(t)} + \frac{\lambda}{2}(w_{(t+1)j}^{(t)} + w_{(t-1)j}^{(t)})}{(1-\lambda)\sum_j^m w_j^{(t)} + \frac{\lambda}{2}\sum_j^m (w_{(t+1)j}^{(t)} + w_{(t-1)j}^{(t)})} \quad (13)$$

224 and the frequency of a female genotypic combination will be:

$$225 \quad \kappa_j^{(t)} = \frac{(1-\lambda)z_j^{(t)} + \frac{\lambda}{2}(z_{(t+1)j}^{(t)} + z_{(t-1)j}^{(t)})}{(1-\lambda)\sum_j^m z_j^{(t)} + \frac{\lambda}{2}\sum_j^m (z_{(t+1)j}^{(t)} + z_{(t-1)j}^{(t)})} \quad (14)$$

226 The simulations and graphics used in the figures were generated with MATLAB

227 (Code available by request).

228

229 **Results**

230 *Gene flow under a partial sex-biased hybrid incompatibility – effective dispersal*

231 The effective dispersal (λ_e) represents the strength of gene flow or introgression of an
232 allele. The λ_e of alleles on different chromosomes are different as shown in Figure 1. Figure 1
233 shows the distribution of λ_e under the influence of an X_1A_2 incompatibility ranging from 0 to
234 1 ($0 \leq \psi \leq 1$, X-axis) that is in a scenario of a mild density-dependent regulation ($r = 0.05$)
235 and $\lambda = 0.1$ (Figure 1A), 0.2 (Figure 1B) and 0.4 (Figure 1C). It is evident that the
236 introgressions of the incompatible loci (X and A) are highly asymmetrical under a weak
237 Haldane's rule. For instance, in the scenario of $\lambda = 0.4$ (Figure 1C), a 10% ($\psi = 0.1$) X_1A_2
238 incompatibility results in a λ_e of X_1 and A_2 about 0.1060 and 0.158 respectively, and a λ_e of X_2
239 and A_1 of 0.440 and 0.366 respectively at the “equilibrated point” (2000 generations). The
240 non-incompatible alleles (X_2 and A_1) have a much higher introgression comparing to their
241 incompatible counterparts (X_1 and A_2). As shown in Supplementary Figure 1, a higher
242 density-dependent regulation extends the differentiation of introgression between the X and A
243 loci. In a scenario when $r = 0$, $\lambda = 0.4$ and $\psi = 0.2$, the λ_e of X_1 and X_2 would be 0.066 and
244 0.220 respectively. However, when r increases to 0.1 in the same scenario, the λ_e of X_1 and X_2
245 would become 0.118 and 0.51 respectively (Supplementary Figure 1A & 1C). Also, the
246 compatible counterparts of the incompatible alleles have a higher tendency to introgress
247 comparing to the alleles at neutral loci when density-dependent regulation is strong. The λ_e of
248 these compatible counterparts can be much higher than the actual λ , but λ_e of a neutral allele
249 is always lower than λ (Figure 1 and Supplementary Figure 1). A strong flow of non-
250 incompatible alleles (X_2 and A_1 in this example) would constitute a strong homogenization
251 force causing the collapse of the genetic barrier. Furthermore, a density-dependent regulation
252 could substantially be negatively correlated with the barrier strength against the neutral flow.
253 As shown in Supplementary Figure 1D, under a relatively strong density-dependent

254 regulation ($r = 0.5$), the introgression of a neutral allele is very close to the scenario with no
255 incompatibility (the reference lines in Supplementary Figure 1D). Interestingly, the trends of
256 λ_e of all alleles plateau long before a full strength BDM incompatibility ($\psi = 1$), suggesting
257 that even a milder X_1A_2 incompatibility, as low as 20% ($\psi = 0.2$), could mount significant
258 impedance on gene flow that is almost comparable to a 100% incompatibility ($\psi = 1$).

259

260 *The effective of partial sex-biased incompatibilities on the cline structures of various*
261 *alleles*

262 Genetic isolation could cause clinal non-coincidence and discordance of alleles in a hybrid
263 zone. I examined the effects of a weak X_1A_2 unidirectional incompatibility on the clinal
264 structure in relation to variations of ψ , λ , and r . Figure 2 shows some clines of alleles in a
265 number of representative scenarios. It can be seen that an X_1A_2 unidirectional incompatibility
266 causes significant clinal non-coincidence and discordance. The cline of a neutral locus is
267 wider, less steep (P_{CI} in Figure 2), and almost symmetrically distributed, but the clines of
268 incompatible loci are steeper, narrower and asymmetrically distributed (P_{X1} and P_{A1} in Figure
269 2). Figure 2A, B and C show the clines caused by a 10% X_1A_2 incompatibility ($\psi = 0.1$). The
270 non-coincidence of clines is rather obvious and significant under the 10% incompatibility but
271 to a lesser extent in comparison with those under a full scale X_1A_2 heterogametic
272 incompatibility ($\psi = 1$), which is shown in Figure 2D, E and F. Figure 2 also shows that a
273 stronger density-dependent regulation produces less steep clines of the Y and neutral C loci,
274 similar to those formed through neutral diffusion (Endler, 1973) (Endler, 1977, Barton &
275 Gale, 1993). The clines of X and A are more asymmetrically distributed, in which the X locus
276 shows the most asymmetry. This suggests that a very weak X_1A_2 incompatibility under a
277 stronger density-dependent regulation could lead to a pronounced asymmetric introgression
278 of X and A loci, but not in the case of Y and C loci. Among all loci, the cline of the X locus is

279 the narrowest and steepest, which could likely facilitate faster divergences of X -linked loci
280 during speciation.

281

282 *The hybrid sink effects of weak incompatibilities*

283 To better appreciate the fitness effect of a weak X_1A_2 heterogametic incompatibility, the
284 density depression in a hybrid zone as a consequence of elimination of inferior hybrids was
285 examined. The zone here acts as a “sink” because the production of inferior hybrids results in
286 an inward net flow of migrants towards the centre of the zone (the hybrid sink effect)
287 (Barton, 1980, Barton & Bengtsson, 1986). Distribution of relative density ($0 \leq \rho \leq 1$) across
288 a hybrid zone is the function of the incompatibility strength (ψ), dispersal rate (λ), and
289 density-dependent regulation (r). Figure 3 shows the distribution of relative density across a
290 hybrid zone in different scenarios at equilibrium. The density distribution in the zone displays
291 an asymmetrical, “V” shape depression.

292 In this 10 deme scenario, if density-dependent regulation is absent ($r = 0$), the lowest
293 depression point is at deme 5; if density-dependent regulation is present ($r = 0.05$ or 0.2), the
294 lowest depression point shifts to further left to deme 4. This suggests that the asymmetrical
295 pressure increases when density-dependent regulation is larger. The density depression is
296 more pronounced when the strength of the incompatibility is higher, density-dependent
297 regulation is lower, or dispersal rate is (λ) is higher (Figure 3). There is a good correlation
298 between the density distribution and the percentages of inferior offspring produced in a
299 hybrid zone in each generation at equilibrium (See Supplementary Figure 2).

300 Next, I examined the relationship between the density depression and the strength of
301 density-dependent regulation (X -axis). Figure 4 shows the equilibrated density of Deme No.5
302 in response to the varying r values with a 5, 10, 30 or 100% incompatibility strength ($\psi =$
303 0.05, 0.1, 0.3 or 1) and 10 or 40% dispersal ($\lambda = 0.1$ or 0.4). A strong density-dependent

304 regulation can almost entirely compensate for the depression caused by an X_1A_2
305 incompatibility (Figure 3 and Figure 4). The analysis here also suggests that when density-
306 dependent regulation is relatively weak, a weak X_1A_2 heterogametic incompatibility ($\psi \ll 1$)
307 could still be a rather efficient barrier and causes a substantial density depression (Figure
308 s3A, 3B and 4). However, if density-dependent regulation is strong and the r value is large (r
309 > 0.2), even a full strength heterogametic incompatibility ($\psi = 1$) would only cause an
310 insignificant density depression (Figure 4). Density-dependent regulation is an important
311 factor in regulating the density and the size of demes in a hybrid zone.

312 **Discussion**

313 The current paper is an attempt to examine the role of a weak BDM incompatibility in a
314 hybrid zone system. It provides a more quantitative account of how “slightly lessened fertility
315 (see ‘Charles Darwin's letters: a selection, 1825-1859’ Darwin & Burkhardt, 1998)” caused by
316 weak sex-biased inferiority (*i.e.* weak Haldane's rule) could contribute to the genetic
317 divergence and potentially the establishment of complete reproductive isolation during
318 speciation. The gene frequency changes and gene flow between diverging populations during
319 speciation are at the heart of population genetics. I found that a weak sex-biased hybrid
320 incompatibility can profoundly affect gene flow past a hybrid zone. A weak, sex-biased BDM
321 incompatibility provides *a*) a significant reinforcement pressure to drive further divergence of
322 population; and *b*) a substantial drive of the asymmetrical flow of incompatible loci (Figures
323 1), which leads to significant clinal non-coincidence and discordance (Figure 2).

324 The impedance of the flow of incompatible genes across a hybrid zone is no surprising.
325 Such gene flow usually results in abrupt clines (Barton & Gale, 1993). It is interesting,
326 however, that such impedance can be achieved through a weak, sex-biased BDM
327 incompatibility. As shown in Figure 1, a weak incompatibility with 10-20% ($\psi = 0.1-0.2$)
328 strength is sufficient to confer a significant reduction of gene flow across a hybrid zone of an
329 incompatible allele. The effective dispersal of most alleles under a 20% incompatibility is
330 close to that of a full strength sex-biased incompatibility (Figure 1). Such reduced gene flow
331 results in characteristic clinal structures in the hybrid zone. The width, steepness and spatial
332 distribution of allele clines (Figure 2) are similar, but to lesser extent, to those under a full
333 strength incompatibility (Wang & Zhao, 2008). Furthermore, a weak compatibility can also
334 cause a substantial density depression in the hybrid zone that is only moderately shallower
335 than a full strength sex-biased incompatibility (Figure 3). In essence, a hybrid zone in the
336 presence of weak sex-biased BDM isolation would act like a filter: it selectively blocks the

337 exchange of incompatible ones (e.g. X_1 and A_2 in an X_1A_2 incompatibility) and at the same
338 time, allows almost free exchange of neutral loci similar to that through neutral diffusion (P_{CI}
339 in Supplementary Figure 1C and 1D). The introgression of non-incompatible alleles, such as
340 the X_2 and A_1 in the case of X_1A_2 incompatibility, would be higher than that of neutral alleles
341 (Supplementary Figure 1C and D). The most affected loci by a weak Haldane's rule are on
342 the X chromosomes. These trends are more pronounced when density-dependent regulation is
343 high.

344 The real question is how relevant these trends are to genetic divergence and speciation. It
345 is conceivable that a hybrid zone (tension zone) with a sex-biased isolation is highly unstable
346 and mobile, because of asymmetric gene flow and incomplete isolation. Maintaining such a
347 hybrid zone would have to involve other selection forces. For instance, a hybrid zone could
348 be stabilized if alleles related to BDM isolation have selective advantages in their own
349 respective localities; or when it coincides with density troughs and/or habitat boundaries with
350 environmental differentiations, which is indeed often the case in nature (Hewitt, 1988, Rice &
351 Hostert, 1993). The population dynamics described in this study may be indicative of how
352 sex-biased BDM incompatibilities is established and preserved during speciation.

353 Studies on diverse taxa have shown that natural selection caused by habitat shifts and
354 environmental changes can lead to extremely rapid genetic divergence and ecological
355 segregation, such as soapberry bugs (Carroll, 1997 #716; Carroll, 2003 #727), threespine
356 sticklebacks (Schluter, 1996, Albert et al., 2008, Berner et al., 2009), cichlids (Barluenga et
357 al., 2006), Neotropical guppies (Reznick et al., 1997), island lizards (Losos et al., 1997), and
358 rainforest passerines (Smith et al., 1997). For instance, after the introduction of an alternative
359 host into North America in less than 100 generations, the "derived-type" soapberry bugs
360 (*Jadera hematoloma*) had evolved epistatic incompatibilities from the "ancestral-type"
361 (Carroll et al., 2003). The "derived-type" and "ancestral-type" were genetically diverged in

362 the feeding morphology, growth rate, survival and fecundity (Carroll et al., 1997). In
363 threespine sticklebacks, the analysis of neutral microsatellites markers indicate that adaptive
364 divergence and partial reproductive isolation often coexist between two parapatric
365 populations (Berner et al., 2009). In these fish, some genomic regions, including the sex-
366 determining chromosome region, have the largest effect on adaptive traits by QTL analysis,
367 suggesting a rapid fixation of adaptive mutations and uneven divergence of different
368 chromosomal regions (Albert et al., 2008); ecological selection also drove rapid evolution of
369 extrinsic postzygotic isolation (Gow et al., 2007) and prezygotic isolation (Boughman et al.,
370 2005) between benthic and limnetic sticklebacks.

371 In recent years, many hotspot genes and mutations have been discovered (Stern &
372 Orgogozo, 2009). The evolutionary changes in the hotspots are often associated with specific
373 adaption (ffrench-Constant et al., 1998, Wichman et al., 1999, Shindo et al., 2005); and/or
374 with sex-biased incompatibility and Haldane's rule in various species pairs (Wittbrodt et al.,
375 1989, Ting et al., 1998, Barbash et al., 2003, Presgraves et al., 2003, Brideau et al., 2006,
376 Masly et al., 2006, Mihola et al., 2009, Phadnis & Orr, 2009, Tang & Presgraves, 2009).
377 These studies support the notion that the rapid evolution of isolating mechanisms is not
378 merely the by-products of genetic drifts or neutral divergence, as many once believed, in
379 environments with high ecological differentiations in sympatry or parapatry (Carroll et al.,
380 1997, Reznick et al., 1997, Orr & Smith, 1998, Wang, 2003, Wang & Zhao, 2008).

381 The interplays between adaptation and reproductive isolation hold the key for the
382 evolution of sexually reproducing organisms (Butlin et al., 2008, Fitzpatrick et al., 2008). In
383 light of the current analysis, one can speculate that in a highly differentiated environment, the
384 adaptive changes in subpopulations would more likely be preserved during speciation, if they
385 happen to cause hybrid inferiority. This mechanism may have led to the dominance of BDM
386 isolation and Haldane's rule. This population dynamics provides a glimpse of how a

387 speciation gene comes into being at an early stage of population divergence. In a
388 megapopulation consisting of many clades with complex environmental differentiations, an
389 adaptive mutation could set the gene up as a hotspot that initiates a runaway evolutionary
390 process toward more complete reproductive isolation. With such dynamics, local adaptation
391 and postzygotic isolation could promote each other during genetic divergence and population
392 differentiation. This model may also be extended to test some controversial issues in
393 evolutionary biology. For instance, whether or not secondary contact is a prerequisite for the
394 formation of hybrid zone and species; whether or not hybrid zones are the sites of
395 'reinforcement' (Dobzhansky, 1940) – the evolution of prezygotic barriers to gene exchange
396 in response to selection against hybrids (Harrison, 1993). These are the fundamental
397 questions in the field of population genetics that remain controversial for many years
398 (Paterson, 1978, 1982; Butlin, 1987, 1989).

399

400

401 **Acknowledgments**

402 I thank Tania Kastelic and Philip Tang for help with English editing.

403 **Figure 1.** The effective dispersal (λ_e) of different alleles in a scenario of $r = 0.05$ with
404 dispersal of (A) $\lambda = 0.1$; (B) $\lambda = 0.2$; and (C) $\lambda = 0.4$. The strength of an X_1A_2 heterogametic
405 incompatibility varies from 0 to 1 (X -axis). The horizontal dotted line in each panel is the
406 reference line, which represents a scenario of no genetic incompatibility between two
407 parental populations.

408

409 **Figure 2.** The non-coincident and discordant clines of the representative loci, X , Y , A and
410 C across a hybrid zone consisting of 10 demes with different density-dependent regulations
411 (r) and barrier strengths (ψ – caused by an X_1A_2 heterogametic incompatibility) at 40%
412 dispersal ($\lambda = 0.4$). (A) $r = 0$, $\psi = 0.1$; (B) $r = 0.05$, $\psi = 0.1$; (C) $r = 0.4$, $\psi = 0.1$; (D) $r = 0$, ψ
413 $= 1$; (E) $r = 0.05$, $\psi = 1$; (F) $r = 0.4$, $\psi = 1$.

414

415 **Figure 3.** The relative density depression in an equilibrated hybrid zone ($t = 2000$)
416 consisting of 10 demes with the various strengths (ψ) of an X_1A_2 heterogametic
417 incompatibility and different density-dependent regulation, (A and D. $r = 0$; B and E. $r =$
418 0.05 ; and C and F. $r = 0.2$). In each panel, the alternate lines from top to bottom represent the
419 strength of an X_1A_2 heterogametic incompatibility of $\psi = 0.05, 0.1, 0.2, 0.3, 0.5$ or 1 .

420

421 **Figure 4.** The equilibrated density distribution in Deme No.5 under different density-
422 dependent regulation in a scenario of 10 demes with different strengths of an X_1A_2
423 heterogametic incompatibility ($\psi = 0.05, 0.1, 0.3$ and 1) and dispersal (A) $\lambda = 0.1$ (B) $\lambda = 0.4$.

424

425 **Figure 5.** The population density over time (generations) in the Deme No.5 with different
426 strength of BDM incompatibility (ψ). From top to bottom, the alternate lines from top to
427 bottom represent a ψ value of $0.05, 0.1, 0.2, 0.3, 0.5$ or 1 , respectively.

428

429 **Supplementary Figure 1.** The effective dispersal (λ_e) of different alleles in scenarios of
430 (A) $r = 0$, (B) $r = 0.05$, (C) $r = 0.1$, and (D) $r = 0.5$ with 40% dispersal ($\lambda = 0.4$) and the
431 strength (ψ) of an X_1A_2 heterogametic incompatibility varying from 0 to 1 (X -axis). The
432 horizontal dotted line in each panel is the reference line representing a scenario of no
433 incompatibility, in which there is no genetic isolation two parental populations.

434

435 **Supplementary Figure 2.** The percentage of inferior offspring under a complete X_1A_2
436 heterogametic incompatibility ($\psi = 1$) in each generation at equilibrium. The variations of
437 parameters are: $r = 0, 0.05, \text{ and } 0.2$; $\lambda = 0.05, 0.2 \text{ and } 0.4$.

438

439 **Supplementary Figure 3.** The time (generations) required for establishing equilibrium
440 under a weak X_1A_2 heterogametic incompatibility. The cutoff of equilibration is set at the 1%
441 collective size of all 10 demes. The hybrid zone with a size change smaller than the cutoff
442 between generations is considered at equilibrium. Here, the strength of the incompatibility
443 (ψ) varies from 0 to 1 (X -axis). Dispersal of 10, 20 and 40% ($\lambda = 0.1, 0.2 \text{ and } 0.4$) are
444 considered. (A) $r = 0$; (B) $r = 0.05$; (B) $r = 0.1$; and (C) $r = 0.5$.

445

446 **References:**

- 447 Albert, A. Y., Sawaya, S., Vines, T. H., Knecht, A. K., Miller, C. T., Summers, B. R.,
 448 Balabhadra, S., Kingsley, D. M. & Schluter, D. 2008. The genetics of adaptive shape
 449 shift in stickleback: pleiotropy and effect size. *Evolution* **62**: 76-85.
- 450 Arnegard, M. E. & Kondrashov, A. S. 2004. Sympatric speciation by sexual selection alone is
 451 unlikely. *Evolution* **58**: 222-37.
- 452 Barbash, D. A., Siino, D. F., Tarone, A. M. & Roote, J. 2003. A rapidly evolving MYB-
 453 related protein causes species isolation in *Drosophila*. *Proc. Natl. Acad. Sci. USA*.
 454 **100**: 5302-5307.
- 455 Barluenga, M., Stolting, K. N., Salzburger, W., Muschick, M. & Meyer, A. 2006. Sympatric
 456 speciation in Nicaraguan crater lake cichlid fish. *Nature* **439**: 719-23.
- 457 Barton, N. & Bengtsson, B. O. 1986. The barrier to genetic exchange between hybridising
 458 populations. *Heredity* **57**: 357-76.
- 459 Barton, N. H. 1980. The hybrid sink effect. *Heredity* **44**: 277-278.
- 460 Barton, N. H. & Gale, K. S. (1993) Genetic analysis of hybrid zones. In: *Hybrid zones and*
 461 *the evolutionary process*, (Harrison, R. G., ed.). pp. 13-45. Oxford University Press,
 462 New York.
- 463 Bateson, W. (1909) Heredity and variation in modern lights. In: *Darwin and Modern Science*,
 464 (Seward, A. C., ed.). pp. 85-101. Cambridge University Press, Cambridge.
- 465 Bengtsson, B. O. (1985) The flow of genes through a genetic barrier. In: *Evolution: essays in*
 466 *honour of John Maynard Smith*, (Greenwood, J. J., Harvey, P. H. & Slatkin, M., eds.).
 467 pp. 31-42. Cambridge Univ. Press, Cambridge, U.K.
- 468 Berner, D., Grandchamp, A. C. & Hendry, A. P. 2009. Variable progress toward ecological
 469 speciation in parapatry: stickleback across eight lake-stream transitions. *Evolution* **63**:
 470 1740-53.
- 471 Boughman, J. W., Rundle, H. D. & Schluter, D. 2005. Parallel evolution of sexual isolation in
 472 sticklebacks. *Evolution* **59**: 361-73.
- 473 Brideau, N. J., Flores, H. A., Wang, J., Maheshwari, S., Wang, X. & Barbash, D. A. 2006.
 474 Two Dobzhansky-Muller genes interact to cause hybrid lethality in *Drosophila*.
 475 *Science* **314**: 1292-5.
- 476 Butlin, R. K., Galindo, J. & Grahame, J. W. 2008. Sympatric, parapatric or allopatric: the
 477 most important way to classify speciation? *Philos Trans R Soc Lond B Biol Sci* **363**:
 478 2997-3007.
- 479 Carroll, S. P., Dingle, H. & Famula, T. R. 2003. Rapid appearance of epistasis during
 480 adaptive divergence following colonization. *Proc Biol Sci* **270 Suppl 1**: S80-3.
- 481 Carroll, S. P., Dingle, H. & Klassen, S. P. 1997. Genetic Differentiation of Fitness-
 482 Associated Traits Among Rapidly Evolving Populations of the Soapberry Bug.
 483 *Evolution* **51**: 1182-1188.
- 484 Coyne, J. A. & Orr, H. A. (1989) Two rules of speciation. In: *Speciation and Its*
 485 *Consequences*, (Otte, D. & Endler, J. A., eds.). pp. 180-207. Sinauer Associates,
 486 Sunderland, MA.
- 487 Coyne, J. A. & Orr, H. A. 1998. The evolutionary genetics of speciation. *Philos. Trans. R.*
 488 *Soc. Lond. B Biol. Sci.* **353**: 287-305.
- 489 Coyne, J. A. & Orr, H. A. 2004. *Speciation*. Sinauer Associates, Sunderland, Mass.
- 490 Darwin, C. & Burkhardt, F. H. 1998. *Charles Darwin's letters : a selection, 1825-1859*,
 491 Canto ed. Cambridge University Press, Cambridge.
- 492 Dieckmann, U. & Doebeli, M. 1999. On the origin of species by sympatric speciation. *Nature*
 493 **400**: 354-7.

- 494 Dieckmann, U., Doebeli, M., Metz, J. A. J. & Tautz, D. (2004) Epilogue. In: *Adaptive*
495 *speciation*, (Dieckmann, U., Doebeli, M., Metz, J. A. J. & Tautz, D., eds.). pp. 380-
496 394 Cambridge studies in adaptive dynamics. Cambridge University Press,
497 Cambridge, UK ; New York.
- 498 Dobzhansky, T. 1940. Speciation as a Stage in Evolutionary Divergence. *The American*
499 *Naturalist* **74**: 312.
- 500 Dobzhansky, T. G. 1937. *Genetics and the origin of species*, 2d. , rev. ed. Columbia
501 University Press, New York.
- 502 Endler, J. A. 1973. Gene flow and population differentiation. *Science* **179**: 243-50.
- 503 Endler, J. A. 1977. *Geographic variation, speciation, and clines*. Princeton University Press,
504 Princeton, N.J.
- 505 French-Constant, R. H., Pittendrigh, B., Vaughan, A. & Anthony, N. 1998. Why are there so
506 few resistance-associated mutations in insecticide target genes? *Philos Trans R Soc*
507 *Lond B Biol Sci* **353**: 1685-93.
- 508 Fitzpatrick, B. M., Fordyce, J. A. & Gavrillets, S. 2008. What, if anything, is sympatric
509 speciation? *J Evol Biol* **21**: 1452-9.
- 510 Fitzpatrick, B. M., Fordyce, J. A. & Gavrillets, S. 2009. Pattern, process and geographic
511 modes of speciation. *J Evol Biol* **22**: 2342-7.
- 512 Gavrillets, S. 1997. Hybrid Zones With Dobzhansky-Type Epistatic Selection. *Evolution* **51**:
513 1027-1035.
- 514 Gourbiere, S. 2004. How do natural and sexual selection contribute to sympatric speciation? *J*
515 *Evol Biol* **17**: 1297-309.
- 516 Gow, J. L., Peichel, C. L. & Taylor, E. B. 2007. Ecological selection against hybrids in
517 natural populations of sympatric threespine sticklebacks. *J Evol Biol* **20**: 2173-80.
- 518 Harrison, R. G. (1993) Hybrids and hybrid zones: historical perspective. In: *Hybrid zones and*
519 *the evolutionary process*, (Harrison, R. G., ed.). pp. 3-12. Oxford University Press,
520 New York.
- 521 Hartl, D. L. & Clark, A. G. 1997. *Principles of population genetics*, 3rd ed. Sinauer
522 Associates, Sunderland, MA.
- 523 Hewitt, G. M. 1988. Hybrid zones-natural laboratories for evolutionary studies. *Trends in*
524 *Ecology & Evolution* **3**: 158-167.
- 525 Laurie, C. C. 1997. The weaker sex is heterogametic: 75 years of Haldane's rule. *Genetics*
526 **147**: 937-51.
- 527 Losos, J. B., Warheitt, K. I. & Schoener, T. W. 1997. Adaptive differentiation following
528 experimental island colonization in *Anolis* lizards. *Nature* **387**: 70-73.
- 529 Masly, J. P., Jones, C. D., Noor, M. A., Locke, J. & Orr, H. A. 2006. Gene transposition as a
530 cause of hybrid sterility in *Drosophila*. *Science* **313**: 1448-50.
- 531 Mihola, O., Trachtulec, Z., Vlcek, C., Schimenti, J. C. & Forejt, J. 2009. A mouse speciation
532 gene encodes a meiotic histone H3 methyltransferase. *Science* **323**: 373-5.
- 533 Muller, H. J. (1940) Bearings of the "*Drosophila*" work on systematics. In: *The new*
534 *systematics*, (Huxley, J. S., ed.). pp. 185-268. Clarendon, Oxford.
- 535 Muller, H. J. 1942. Isolating mechanisms, evolution and temperature. *Biological Symposia* **6**:
536 71-125.
- 537 Orr, H. A. 1996. Dobzhansky, Bateson, and the genetics of speciation. *Genetics* **144**: 1331-5.
- 538 Orr, M. R. & Smith, T. B. 1998. Ecology and speciation. *Trends in ecology & evolution* **13**:
539 502-506.
- 540 Phadnis, N. & Orr, H. A. 2009. A single gene causes both male sterility and segregation
541 distortion in *Drosophila* hybrids. *Science* **323**: 376-9.

- 542 Presgraves, D. C., Balagopalan, L., Abmayr, S. M. & Orr, H. A. 2003. Adaptive evolution
543 drives divergence of a hybrid inviability gene between two species of *Drosophila*.
544 *Nature* **423**: 715-9.
- 545 Reznick, D. N., Shaw, F. H., Rodd, F. H. & Shaw, R. G. 1997. Evaluation of the Rate of
546 Evolution in Natural Populations of Guppies (*Poecilia reticulata*). *Science* **275**: 1934-
547 1937.
- 548 Rice, W. R. & Hostert, E. E. 1993. Laboratory Experiments on Speciation: What Have We
549 Learned in 40 Years? *Evolution* **47**: 1637-1653.
- 550 Schluter, D. 1996. Ecological Causes of Adaptive Radiation. *The American Naturalist* **148**:
551 S40.
- 552 Shindo, C., Aranzana, M. J., Lister, C., Baxter, C., Nicholls, C., Nordborg, M. & Dean, C.
553 2005. Role of FRIGIDA and FLOWERING LOCUS C in determining variation in
554 flowering time of *Arabidopsis*. *Plant Physiol* **138**: 1163-73.
- 555 Slatkin, M. 1973. Gene flow and selection in a cline. *Genetics* **75**: 733-56.
- 556 Smith, T. B., Wayne, R. K., Girman, D. J. & Bruford, M. W. 1997. A Role for Ecotones in
557 Generating Rainforest Biodiversity. *Science* **276**: 1855-1857.
- 558 Stern, D. L. & Orgogozo, V. 2009. Is genetic evolution predictable? *Science* **323**: 746-51.
- 559 Tang, S. & Presgraves, D. C. 2009. Evolution of the *Drosophila* nuclear pore complex results
560 in multiple hybrid incompatibilities. *Science* **323**: 779-82.
- 561 Ting, C. T., Tsauro, S. C., Wu, M. L. & Wu, C. I. 1998. A rapidly evolving homeobox at the
562 site of a hybrid sterility gene. *Science* **282**: 1501-4.
- 563 Van Doorn, G. S. 2004. Sympatric speciation by sexual selection: a critical reevaluation. *Am.*
564 *Nat.* **163**: 709-25.
- 565 van Doorn, G. S., Edelaar, P. & Weissing, F. J. 2009. On the origin of species by natural and
566 sexual selection. *Science* **326**: 1704-7.
- 567 Wang, R. X. 2003. Differential strength of sex-biased hybrid inferiority in impeding gene
568 flow may be a cause of Haldane's rule. *J. Evol. Biol.* **16**: 353-361.
- 569 Wang, R. X. & Zhao, Y. L. 2008. Differential barrier strength and allele frequencies in hybrid
570 zones maintained by sex-biased hybrid incompatibilities. *Heredity* **100**: 326-336.
- 571 Wichman, H. A., Badgett, M. R., Scott, L. A., Boulianne, C. M. & Bull, J. J. 1999. Different
572 trajectories of parallel evolution during viral adaptation. *Science* **285**: 422-4.
- 573 Wittbrodt, J., Adam, D., Malitschek, B., Maueler, W., Raulf, F., Telling, A., Robertson, S. M.
574 & Scharl, M. 1989. Novel putative receptor tyrosine kinase encoded by the
575 melanoma-inducing Tu locus in *Xiphophorus*. *Nature* **341**: 415-21.
- 576 Wright, S. 1988. Surfaces of Selective Value Revisited. *The American Naturalist* **131**: 115-
577 123.
- 578 Wu, C.-I. 2001. The genic view of the process of speciation. *J. Evol. Biol.* **14**: 851-65.
- 579 Wu, C.-I. & Davis, A. W. 1993. Evolution of postmating reproductive isolation: the
580 composite nature of Haldane's rule and its genetic bases. *Am. Nat.* **142**: 187-212.

Figure 1

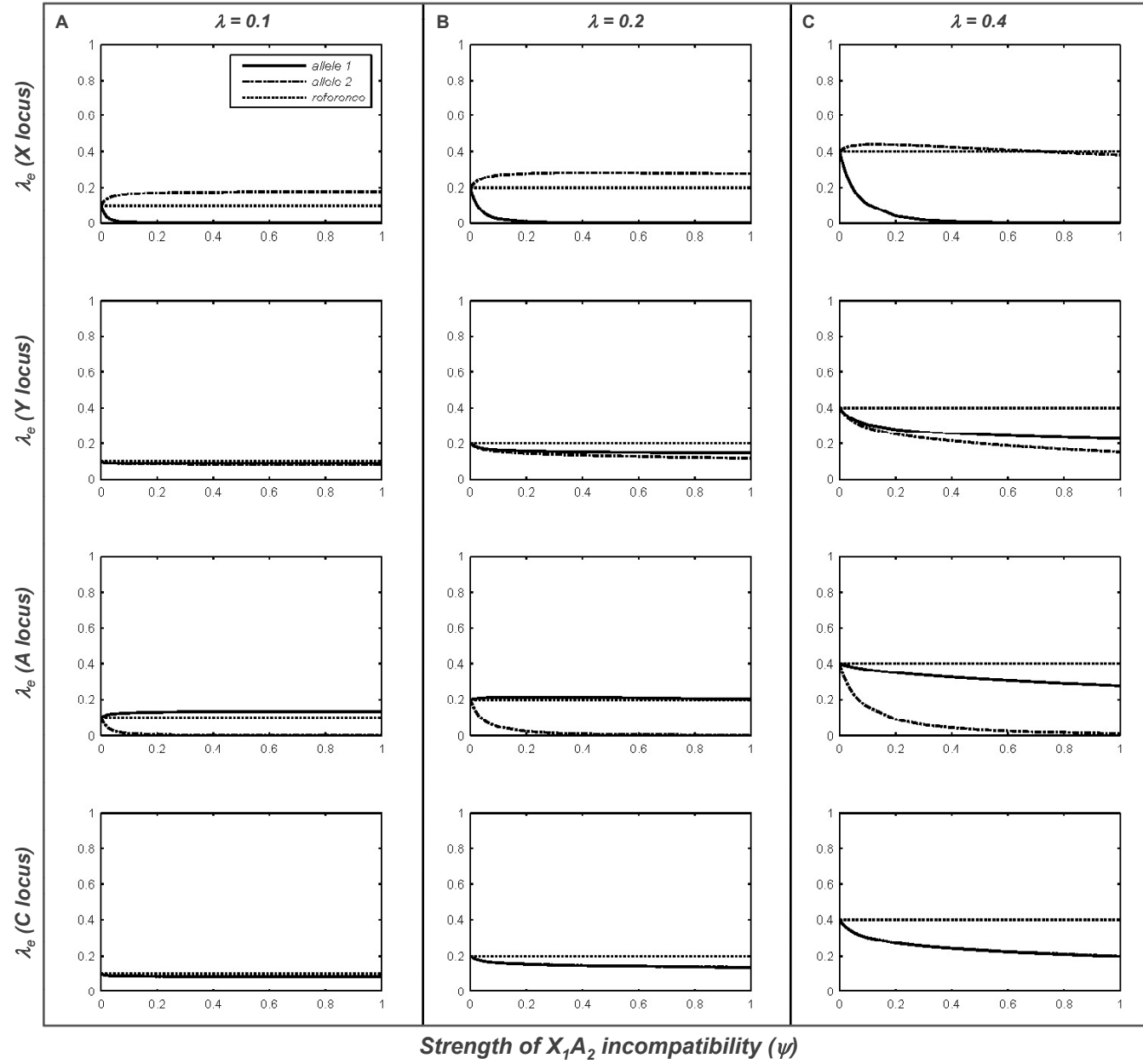


Figure 1

Figure 2

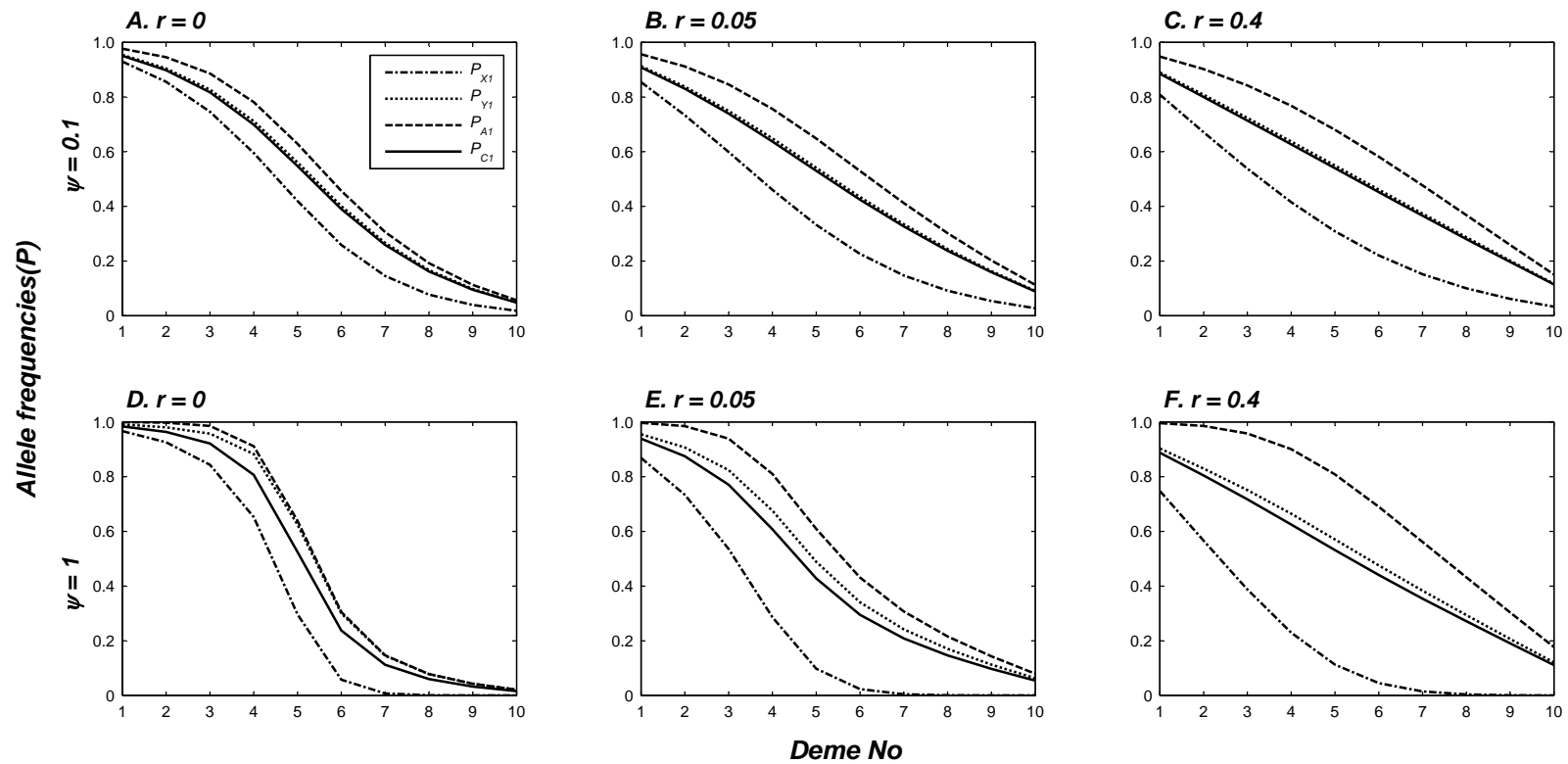


Figure 3

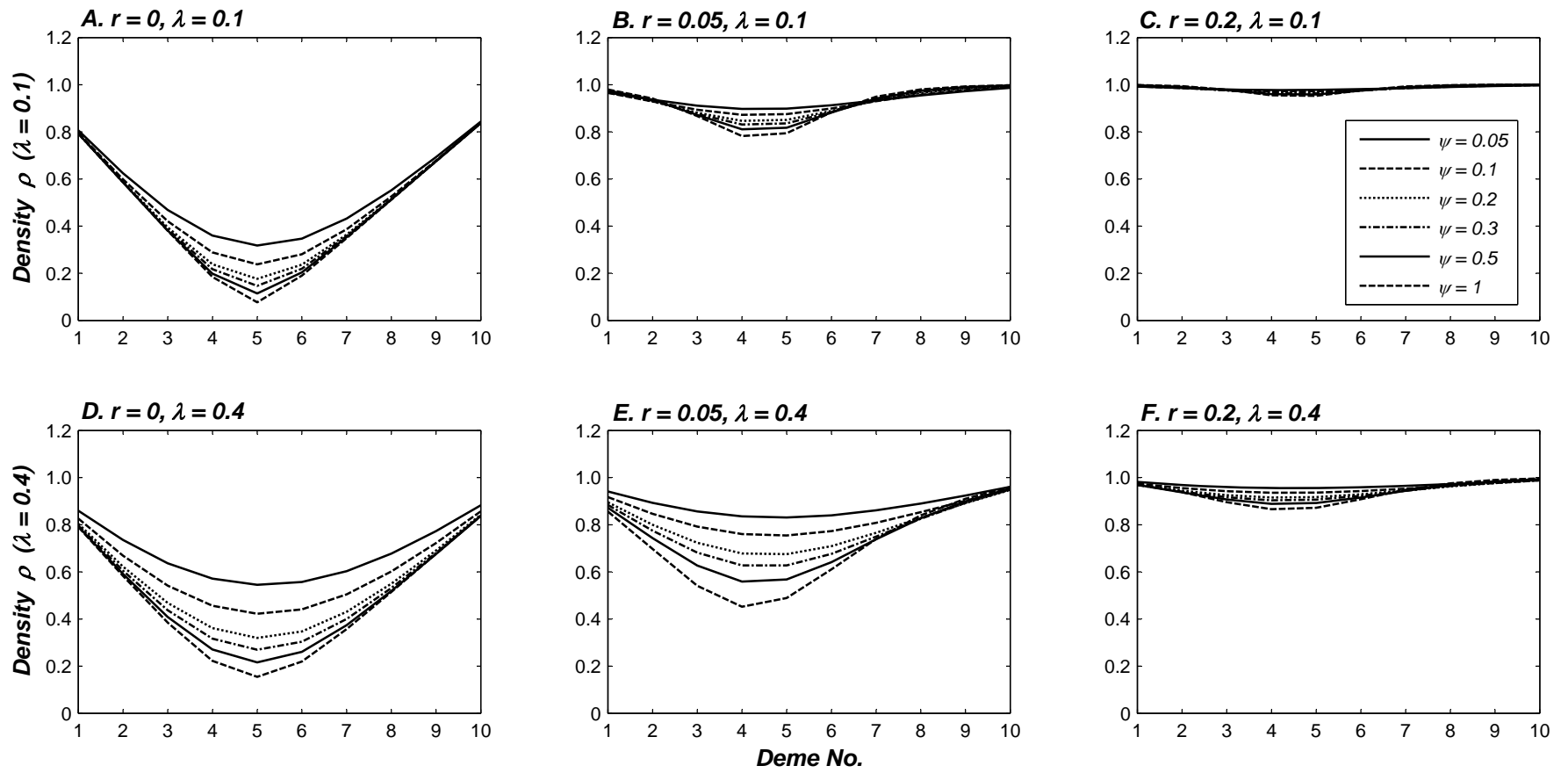


Figure 4

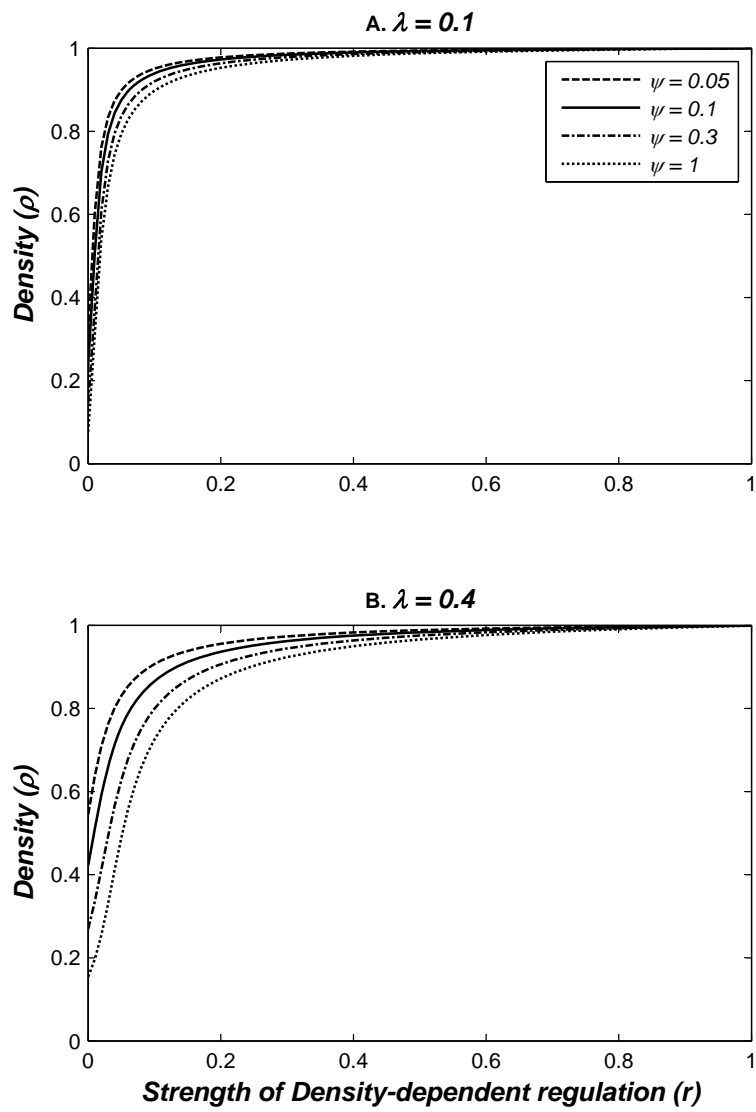
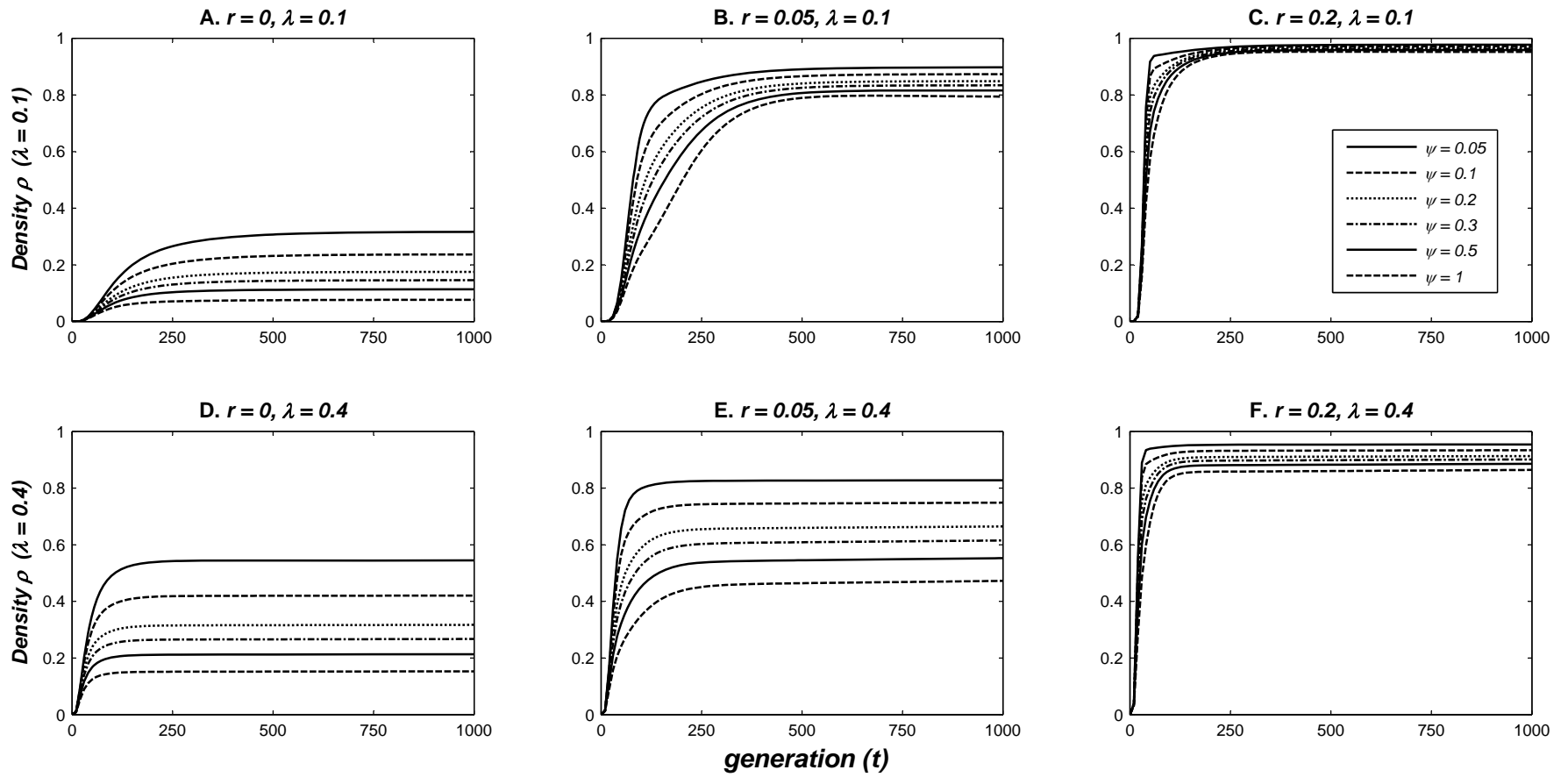
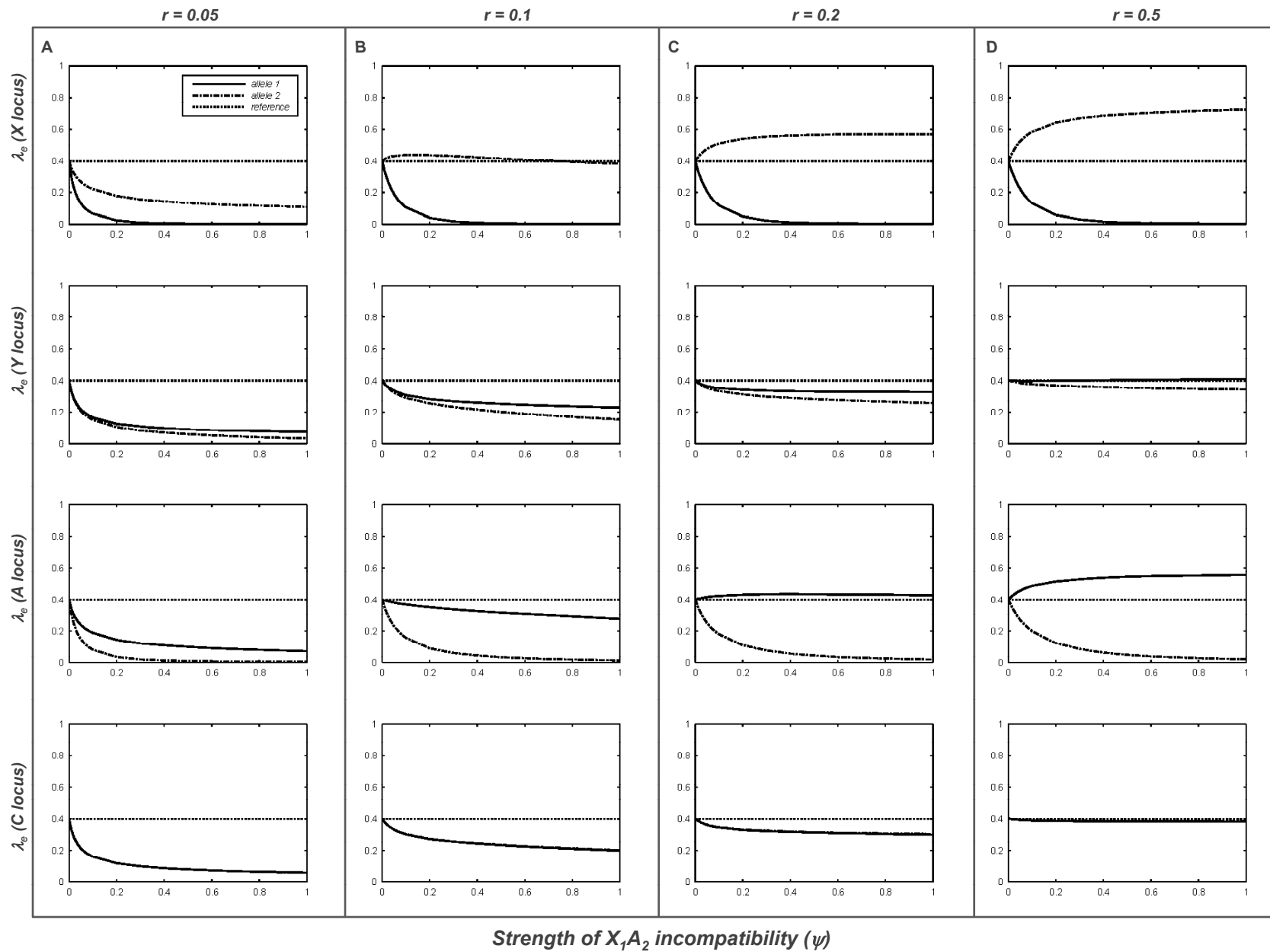


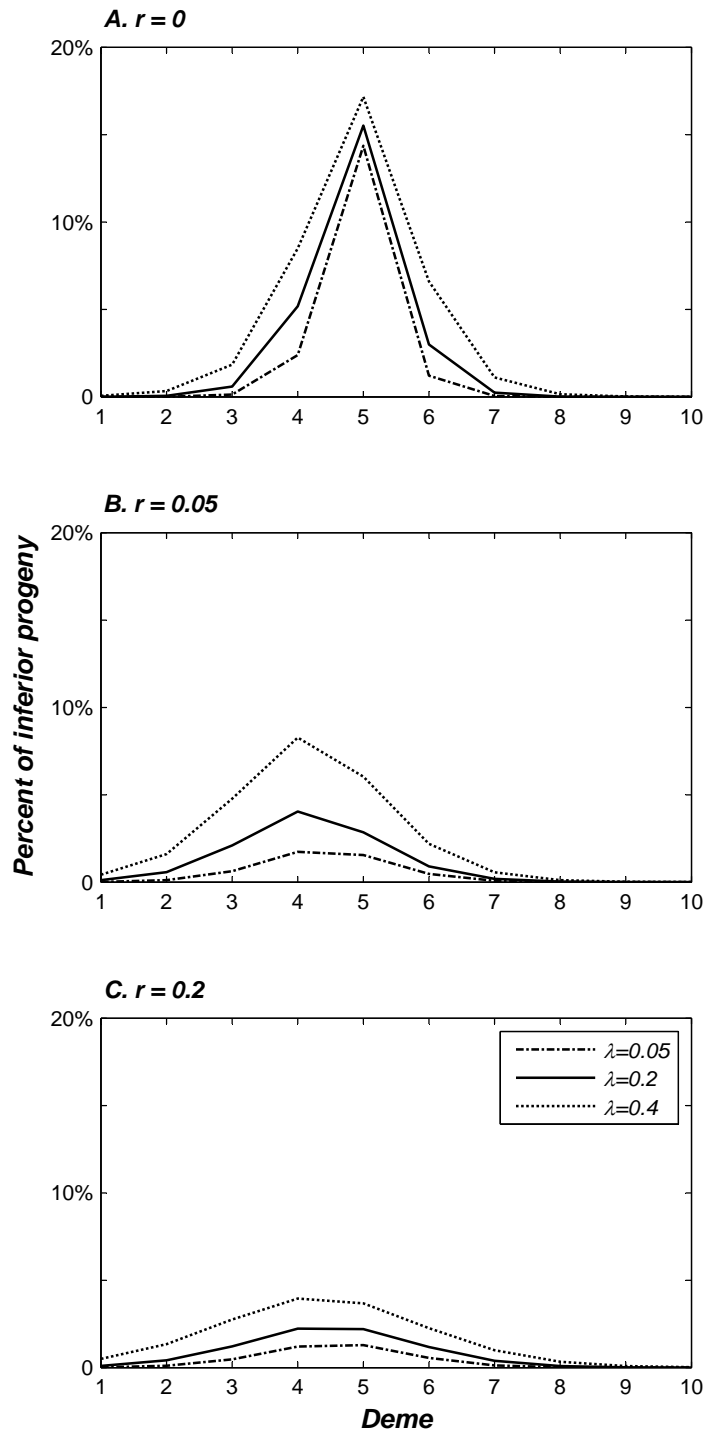
Figure 5





Supplementary Figure 1

Supplementary Figure 2



Supplementary Figure 3

